



Available online at www.sciencedirect.com

ScienceDirect

Procedia Structural Integrity 7 (2017) 3-10



3rd International Symposium on Fatigue Design and Material Defects, FDMD 2017, 19-22 September 2017, Lecco, Italy

Fatigue behaviour of additively-manufactured metallic parts

Nima Shamsaei* and Jutima Simsiriwong

Laboratory for Fatigue & Additive Manufacturing Excellence (FAME), Department of Mechanical Engineering, Auburn University, Auburn, AL 36849, USA

Abstract

An overview on recent research efforts is presented to obtain an understanding on the fatigue behaviour and failure mechanisms of metallic parts fabricated via powder-based additive manufacturing (AM) processes, including direct energy deposition (DED) and powder bed fusion (PBF) methods, utilizing either laser or electron beam as an energy source. Some challenges inherent to characterizing the mechanical behaviour of AM metals under cyclic loading are discussed, with emphasis on the effects of residual stresses on their fatigue resistance. In addition, an aspect pertaining to the structural integrity of AM parts relating to their fatigue behaviour at very high cycles is presented and compared with those of the conventionally-manufactured counterparts.

Copyright © 2017 The Authors. Published by Elsevier B.V. Peer-review under responsibility of the Scientific Committee of the 3rd International Symposium on Fatigue Design and Material Defects.

Keywords: Additive manufacturing (AM); Fatigue; Microstructure; Failure mechanisims; Residual stress; Very high cycle fatigue

1. Introduction

Additive manufacturing (AM) is gaining significant attention in various industries, such as aerospace, automotive, and biomedical, due to its many unique advantages specifically the ability to fabricate customized and complex parts that are often unobtainable with conventional manufacturing methods¹⁻³. Despite the fact that AM technologies have been continued to demonstrate many potentials, the mechanical behaviour, and in particular the fatigue behaviour, of

^{*} Corresponding author. Tel.: +1-334-844-4839; Fax: +1-334-844-3307. E-mail address: shamsaei@auburn.edu

AM parts are not yet fully realized. This lack of understanding creates a barrier against AM technologies to be adopted in many load-bearing, fracture-critical applications⁴⁻⁵.

The presence of material anomalies (i.e., process-driven defects such as lack of fusion voids, entrapped gas pores, etc.) and microstructural properties and heterogeneity resulted from directional heat transfer during AM process can significantly affect the mechanical behaviour of AM parts especially under cyclic loading⁶⁻⁹. For laser-powder bed fusion (L-PBF) and direct laser deposition (DLD) processes, two commons manufacturing-induced defects, including (1) lack of fusion (LOF) voids due to unconsolidated partially-/un-melted powder particles, and (2) pores caused by the entrapped gas, are generally observed¹⁰⁻¹⁴. Since they can serve as micro-notches that cause stress concentrations and local plastic deformations within the material, fatigue cracks are typically initiated from these process-induced defects, which are considered to be the main contributors to the lower fatigue resistance of AM parts, as compared to their conventionally-built counterparts. By employing the hot isostatic pressing (HIP), a post-manufacturing treatment at combined high pressure and high temperature, process-induced internal defects can be reduced which consequently strengthens the fatigue resistance. Nonetheless, the effectiveness of HIP in removing defects from AM parts greatly depends on the material as well as the chosen HIP parameters¹⁵. The surface-connected and near surface voids may still exist in HIPed parts as they cannot be removed by this process¹⁶.

Other challenges that may significantly affect the fatigue resistance of AM parts include the condition of surface finish and design parameters (i.e., build orientation, process time interval, size, geometry, etc.), which potentially influence the degree of similitude between the mechanical properties of laboratory specimens and those of actual AM parts. These topics have been comprehensively discussed in some previous reviews^{7,13}.

Beside the aforementioned factors, other important aspects related to the fatigue performance of AM parts, such as the influence of residual stresses and very high cycle fatigue behaviour, need further discussion. In this paper, the fatigue behaviour and failure mechanisms of AM parts related to these topics are discussed based on the recent publications in the literature.

2. Effect of residual stresses

Residual stresses are commonly classified into three types, namely types I, II, and III, depending on the length scale over which they equilibrate within a material. Type I residual stresses (i.e., stresses in macro-scale) extend over large distances and play a significant role in distortion of material. On the other hand, types II and III residual stresses are those that occur between grains at micro-scale, and inside of a grain around dislocations and crystal surfaces at atomic-scale, respectively, due to different phases in the material ¹⁷⁻¹⁸. In this paper, some recent works involving the influence of type I residual stresses on the fatigue behaviour of AM parts are discussed.

Residual stresses are generally induced throughout AM parts during fabrication due to several factors, including the inherent rapid heating/cooling rates, significant spatially varied thermal distribution, and repeated tempering during subsequent laser-deposition process³. The presence of residual stresses often leads to localized deformations that can extensively impact the strength and fatigue resistance of parts¹⁹⁻²¹, or possibly resulting in distortion (i.e., loss of near-net shape geometries) and even failure of parts during fabrication²². In addition, several studies have indicated that the magnitude and pattern of residual stress within AM parts are commonly affected by various aspects, such as process parameters (e.g., scanning pattern, laser power, beam transverse speed, etc.), part geometry, phase transformation, as well as the material properties (e.g., modulus of elasticity, yield strength, thermal conductivity, and coefficient of thermal expansion)^{21,23-24}.

In intermediate and long-life fatigue applications, compressive residual stresses in parts are often desired due to beneficial effects in delaying the crack formation and its growth, typically resulting in an enhanced fatigue resistance. On the other hand, tensile residual stresses facilitate crack opening and propagation from the surface, reducing the fatigue strength of the material²⁵. Common approaches to weaken the tensile residual stresses in AM parts during fabrication are to lower the local thermal gradient by adjusting the process parameters, maintaining optimal melt pool size, or pre-heating of the build plate^{26,18}. Besides optimizing the scan strategies, the residual stress can also be reduced by utilizing post-build heat treatment²⁷⁻²⁸, or mechanical treatments such as shot-peening or surface rolling^{29,30} to relieve internal stresses in AM parts.

By comparing the AM processes for metallic materials with different energy sources (e.g., electron beam versus laser), parts fabricated via electron beam process are less susceptible to residual stress since the processes are typically performed in build chamber at very high temperature, ranging from 600 to 700 °C. An exposure to this temperature for a prolonged period can result in stress relieving during fabrication, at least for titanium alloys³¹.

Relatively few studies have been performed to obtain the effect of residual stress on fatigue resistance of metallic parts manufactured via electron beam-based AM processes^{30,32}. In Edwards et al.³⁰, the mechanical behaviour under cyclic loading for electron beam melting (EBM) Ti-6Al-4V ELI fabricated using various build orientations was investigated. Compressive residual stresses were observed at the bottom (i.e., initial build layers) of the as-built specimen, while tensile residual stresses were induced along the top of the specimen. Nonetheless, after approximately 30 µm depth into the specimen's surface, minimum residual stresses (nearly zero) were measured³⁰.

Force-controlled fatigue experiments were performed on flat EBM specimens with rectangular cross section at stress ratio, R, of -0.2. Figure 1(a) illustrates the fatigue behaviour of EBM Ti-6Al-4V ELI built in horizontal direction under different mechanical post-processing conditions; as-built, machined, and machined - peened with 0.006A intensity and 100% coverage. In addition, the stress-life fatigue data for wrought Ti-6Al-4V subjected to cyclic loading with R = 0.1 were also superimposed in this figure strength in Fig. 1(a) is represented in term of σ_{eff} , which is defined as the effective maximum value of the applied stress for cyclic loading with R = -1. The σ_{eff} value for Ti-6Al-4V was obtained using the following relationship³⁴⁻³⁵.

$$\sigma_{eff} = \sigma_{max} \left(\frac{1-R}{2}\right)^{0.28} \tag{1}$$

where σ_{max} is the maximum applied stress. The exponent of 0.28 in Eq. (1) was derived based on the fatigue data for conventionally-fabricated Ti-6Al-4V material subjected to uniaxial cyclic loading with stress ratio ranging from -0.5 to 0.5³⁵.

As displayed in Fig. 1(a), although the horizontally-built EBM specimens exhibited significantly lower fatigue strength than the wrought counterpart, machining noticeably improved the fatigue resistance of AM specimens. However, the combination of machining and peening did not affect the results and comparable fatigue lives to as-built specimens in intermediate and low cycle fatigue (LCF) regions were achieved for machined and peened specimens. Near-surface porosity defects were found to initiate fatigue cracks in specimens subjected to machining and machining- peening treatments³⁰.

While peening is intended to induce the beneficial compressive residual stresses into the part's surface, it also deteriorates the surface quality of the part. A peened surface generally has high surface roughness, which is commonly known to be one of the most detrimental factors influencing the fatigue resistance, specifically for AM metallic parts. For horizontally-built EBM Ti-6Al-4V specimens, whose major axes of internal defects (i.e., LOF voids) are typically parallel to the loading direction, resulting in some resistance to crack initiation, high surface roughness may have more impact on the fatigue strength as compared to the effect of defects. These findings, as depicted in Fig. 1(a), suggest further investigation to obtain a better understanding of the fatigue behavior of machined-peened AM specimens fabricated in horizontal direction.

The influence of residual stress on fatigue properties of EBM Ti-6Al-4V with various stress-relief post-fabrication thermal treatments has been recently investigated³². Specimens were vertically-built and subjected to either (1) stress relieving heat treatment at 650 °C for 5 hours in air prior to furnace cooling, or (2) HIPing. The authors reported no significant residual stresses (within two standard errors of zero) in specimens in either heat treatment, or the as-built condition.

Figure 1(b) presents the comparison of fatigue strength in term of σ_{eff} for EBM Ti-6Al-4V and the wrought counterpart. Fatigue data for wrought material presented in this figure was obtained from force-controlled cyclic tests with R = 0.1. Force-controlled fatigue experiments conducted on EBM specimens revealed that the fatigue behaviour of as-built and stress-relieved specimens were similar, which can be attributed to the minimum residual stresses induced in EBM specimens during fabrication. On the other hand, HIPed specimens exhibited improved fatigue resistance, comparable or superior to the wrought counterpart, especially in HCF region. The scanning electron microscopy (SEM) analysis indicated that fatigue cracks in all as-built and stress-relieved specimens were initiated

from voids due to partially-melted powder, while these defects were not found at fatigue crack initiation sites of HIPed specimens³².

Furthermore, the data for vertical EBM Ti-6Al-4V specimens in as-built, machined, and machined-peened conditions³⁰ are also included in Fig. 1(b). As seen, as-built specimens from Hrabe et al.³² appear to exhibit superior fatigue strength relative to those in as-built condition from Edwards et al.³⁰ The differences in fatigue behavior between the two studies may be attributed to process parameters variation. Nonetheless, machining and peening process improved the fatigue resistance of Ti-6Al-4V specimens in Edwards et al.³⁰ to be comparable to as-built specimens in Hrabe et al.³² This possibly demonstrates the effectiveness of post-manufacturing mechanical treatment over the stress relieving heat treatment to enhance fatigue resistance of AM parts.

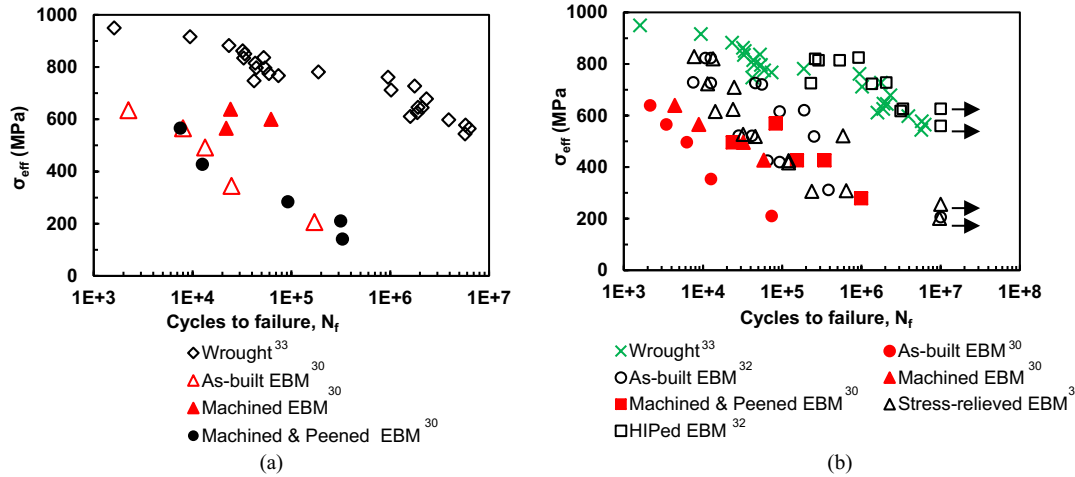


Fig. 1. Comparison of fatigue data for wrought and EBM Ti-6Al-4V ELI fabricated in (a) horizontal and (b) vertical directions, and undergone various post-processing mechanical and thermal treatments. Arrow indicate runout data.

Since laser-based AM processes such as DLD or L-PBF are typically carried out in an inert environment chamber at lower temperatures as compared to electron beam-based processes, the influence of residual stresses on the mechanical properties of the laser-based AM materials should be of concerned. An increase of residual stress for DLD Ti-6Al-4V and AISI 316 SS has been reported as the build height increases (i.e., larger number of layers), along the direction normal to the build plate^{21,36-37}. Furthermore, a variation of residual stresses within the build plane for DLD has been observed along the laser scanning path; lower value at the starting location and larger at the end of the scanning location, and being tensile at the edge of the part and compressive at the center³⁸.

Zhang and co-workers²⁹ investigated the effect of ultrasonic nanocrystal surface modification, which is similar to a peening process, on the residual stress to improve the fatigue performance of L-PBF Ti-6Al-4V. The specimens were fabricated using the direct metal sintering technique and subjected to rotary bending cyclic loading at R = -1. The existed tensile residual stresses were converted to compressive residual stresses, particularly at < 100 µm depth into the surface. By weaken the tensile residual stresses along both the laser scanning direction and build direction using the ultrasonic surface treatment, the fatigue strength of L-PBF Ti-6Al-4V significantly improved, especially for specimens that were treated using lower rotation speeds. Slower rotation speed of the specimens resulted in greater peened surface, which could lead to increased compressive residual stresses and surface hardness, and ultimately fatigue resistance²⁹. The effect of residual stresses on fatigue performance for L-PBF Ti-6Al-4V has also been reported in Leuders et al.²⁷, where stress relieving thermal treatment (800 °C for 2 hours in argon environment, or 1050 °C for 2 hours in vacuum environment) was found to significantly improve the fatigue resistance. Tensile residual stresses were initially observed on the as-built specimens' surface and up to 100 µm depth in both build direction and laser scanning direction. After heat treatment, a majority of residual stresses in the specimens was removed²⁷.

Another study involving the effect of residual stresses on fatigue behaviour of AM Ti-6Al-4V parts fabricated using L-PBF process is by Edward and Ramulu³⁹. Flat L-PBF Ti-6Al-4V specimens were built in horizontal and vertical directions, prior to being tested under cyclic loading in either as-built or machined conditions, without any

post-manufacturing heat treatment. Initial assessment of residual stresses was carried out on two specimens with different geometries, so called short/wide specimen and tall/narrow specimen. The short/wide specimens were fabricated in the orientation parallel to the build platform, representing the horizontal specimen, while tall/narrow specimens were built in the vertical orientation. Tensile residual stresses were observed up into approximately 50 µm depth of short/wide specimen's top and bottom surfaces, while they were found to be present deeper into the top and bottom surfaces of tall/narrow specimen³⁹.

The comparison of fatigue strength for as-built and machined L-PBF Ti-6Al-4V specimens fabricated in horizontal and vertical directions subjected to R = -0.2 test condition as well as wrought Ti-6Al-4V is depicted in Fig. 2. The data displayed in this figure was corrected for the mean stress using Eq. (1). In general, horizontal specimens were found to exhibit greater fatigue resistance, withstanding approximately 60% higher fatigue strength as compared to the vertical specimens³⁹. Since the sub-surface defects directionality are directly influenced by part build orientation, vertical specimens are more susceptible to higher stress concentrations around their internal defects, resulting in less resistance to crack initiation as compared to horizontal specimens. Nonetheless, the fatigue performance for horizontal L-BPF specimens is still significantly lower than wrought material.

Some improvement on the fatigue strength, in particularly in HCF region, of the horizontal L-PBF Ti-6Al-4V specimens after machining can be displayed in this figure. In contrary, minimum enhancement of fatigue strength was reported for vertically-built specimens. Since tensile residual stresses existed deeper into the surface of the tall/narrow specimen (i.e., vertical specimens) as compared to the short/wide specimen (i.e., horizontal specimens), tensile residual stresses may still be present in the vertical specimens in machined condition. In addition, by machining to reduce the tensile residual stresses on the surface in order to strengthen the fatigue resistance of AM specimens, the sub-surface defects such as LOFs and entrapped gas pores were also brought to the specimen's surface that could serve as fatigue crack initiation sites and accelerate the fatigue failure. This particularly affected the fatigue strength of specimens resulting in shorter or similar fatigue lives after machining.

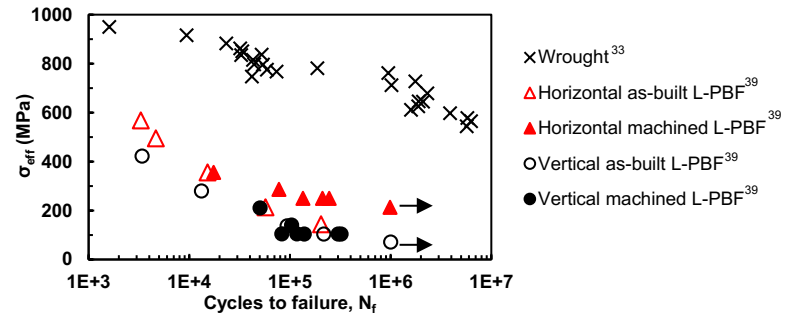


Fig. 2. Comparison of fatigue strengths for wrought and L-PBF Ti-6Al-4V fabricated in horizontal and vertical directions in as-built and machined conditions. Arrows indicate runout data.

In contrary to the fatigue results from various studies present thus far, stress relieving heat treatment may not always lead to the improved fatigue life of AM parts. This finding has been demonstrated by Sterling et al. 10 for Ti-6Al-4V, fabricated via Laser Engineered Net Shaping (LENS), a DLD process. In their study, the DLD specimens were machined and undergone post-build stress relieving heat treatment, at 1050 °C for 2 hours in argon environment, prior to being subjected to fully-reversed strain-controlled cyclic loading. Based on a strain-life approach, shorter fatigue lives in LCF region, and comparable lives in HCF region were reported for heat-treated specimens, relative to specimens without any heat treatment. The reduced fatigue resistance for heat-treated DLD specimens was most likely due to the compressive residual stresses, specifically around pores, that were removed as a result of heat treatment 10.

3. Very high cycle fatigue behaviour

Many components in aerospace and automotive applications, such as engine components and turbine blades, are commonly subjected to cyclic loadings at very high frequency during their service lifetime in which they are required to operate over long periods, exceeding a million cycles⁴⁰. Historically, due to the constraints of conventional fatigue test machine, fatigue-life data of most materials in the literature are typically limited to less than 10⁷ cycles. In the

instance where the data exhibit a nearly horizontal asymptote between 10^6 to 10^7 cycles, then it can be presumed that a fatigue limit of the material exists⁴¹. However, in contrary to the assumption that ferrous alloys exhibit fatigue limit, the material failure under cyclic loading has been reported beyond 10^7 cycles⁴²⁻⁴³. Non-ferrous metallic materials, such as titanium or aluminium, which are preferred in structural applications, do not exhibit a fatigue limit as their stress-life response tends to continuously decrease at a slow rate at greater number of cycles (> 10^7 cycles)⁴⁴.

Performing the experimental studies to obtain the understanding of the materials' fatigue behaviour in very high cycle fatigue (VHCF) regime (i.e., $N_f > 10^7$ cycles) is extremely expensive from the time and cost perspective. Only a fraction of fatigue studies in the literature have been dedicated to investigate mechanical behaviour of AM materials at gigacycle, as well as the corresponding failure mechanisms⁴⁶⁻⁴⁸, which are known to be considerably different from HCF regime (i.e., $10^3 < N_f < 10^6$)⁴⁵.

The effect of build platform heating on the fatigue behaviour in VHCF regime was investigated for L-PBF AlSi12^{46,48}. The experiment was carried out using an ultrasonic fatigue testing method with R = -1, and applied frequency of 20 kHz. Test specimens were vertically fabricated, machined, and underwent the stress relieving heat treatment. Figure 3 displays the fatigue experimental results in both HCF and VHCF regimes for L-PBF AlSi12. In addition, due to the lack of fatigue data for VHCF regime for AlSi12 manufactured using conventional methods, gigacycle fatigue data for cast AlSi7Mg⁴⁹, which has a similar chemical composition but slightly lower Si %wt as compared to AlSi12, under R = -1 and frequency of 19 kHz test condition were superimposed in this figure. By continuously pre-heating the base plate to 200 °C during part fabrication, a beneficial effect on fatigue resistance for L-PBF AlSi12 in VHCF regime was observed, as displayed in Fig. 3.

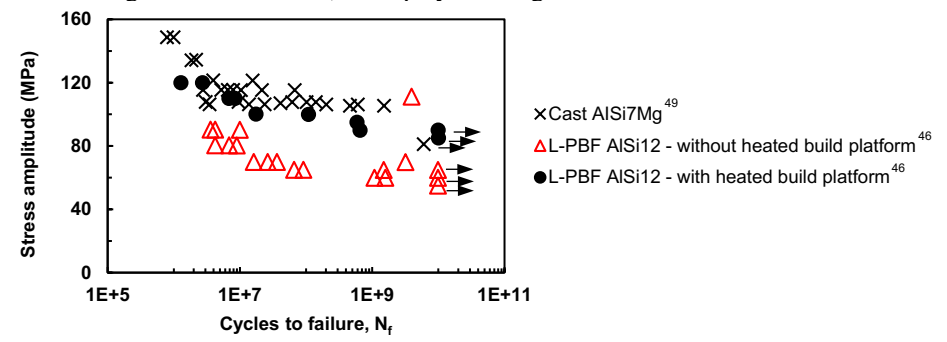


Fig. 3. Comparison of fatigue strengths in high cycle fatigue and very high cycle fatigue regimes for cast AlSi7Mg and L-PBFAlSi12 fabricated with and without heated build platform. Arrows indicate runout data.

By utilizing the build platform heating, lower thermal gradients are experienced within the part which allow dendrites to grow (\sim 0.56 µm average in width, as compared to \sim 0.35 µm for specimens without heated build platform)⁴⁸. The Si precipitates formation was also observed in the specimens with heated build platform due to the reduced cooling/solidification rates, resulting in a microstructural refinement and consequently enhanced fatigue resistance. Moreover, build platform heating was reported to decrease the porosity (\sim 0.25% porosity percentage versus \sim 0.12%) due to the degassing resulting from additional heating. Surface and near-surface pores were observed to serve as crack initiation sites for specimens with heated base plate, while multiple near-subsurface defects due to un-melted powder particles were found to be responsible for crack initiation in specimens without heated build platform⁴⁸. From Fig. 3 it appears that heating the build platform, by eliminating un-melted powder particles, can improve the fatigue resistance of L-PBF AlSi12 in VHCF regime to be somewhat comparable to the one of the cast AlSi7Mg.

Crack initiation mechanisms in L-PBF and EBM Ti-6Al-4V in VHCF regime were investigated in Günther et al. ⁴⁷ The L-PBF specimens were fabricated in vertical direction on a heated build platform, and subjected to either heat treatment to reduce residual stress or HIP. Since the residual stresses in EBM specimens were expected to be minimum, no post-build thermal treatment was performed on them. All specimens were machined and polished to minimize the surface roughness, and ultrasonic fatigue tests were conducted at 19 kHz frequency and R = -1. The experimental results of L-PBF and EBM specimens are presented in Figs. 4(a) and 4(b), respectively. The fatigue data of wrought Ti-6Al-4V⁵⁰ at VHCF regime is also included in this figure. Comparable fatigue lives for L-PBF Ti-6Al-4V specimens with heat treatment and EBM specimens were reported, while L-PBF HIPed specimens exhibited substantially enhanced fatigue resistance, nearly exceeding that of its wrought counterpart, as displayed in Fig. 4.

Generally, two different types of failure in VHCF regime have been observed for conventionally processed materials, including titanium alloy. Fatigue cracks are typically initiated from surface and sub-surface for up to 10^6 cycles and beyond 10^7 cycles, respectively⁵¹. Similar observation was also reported for both L-PBF and EBM Ti-6Al-4V⁴⁷. For non-HIPed specimens, manufacturing-induced defects, including pores caused by entrapped gas and LOF voids, were the main contributor for the fatigue failure in these specimens. The location (i.e., surface or sub-surface) of these defects that are responsible for crack initiations in non-HIPed specimens was not reported. On the other hand, cracks were found to initiate from a single α -phase grain or clusters of α -phase in L-PBF HIPed specimens⁴⁷. This observation implies that the employed HIP process was able to remove all the LOF voids and entrapped gas pores in L-PBF Ti-6Al-4V specimens, thus enhancing their fatigue resistance.

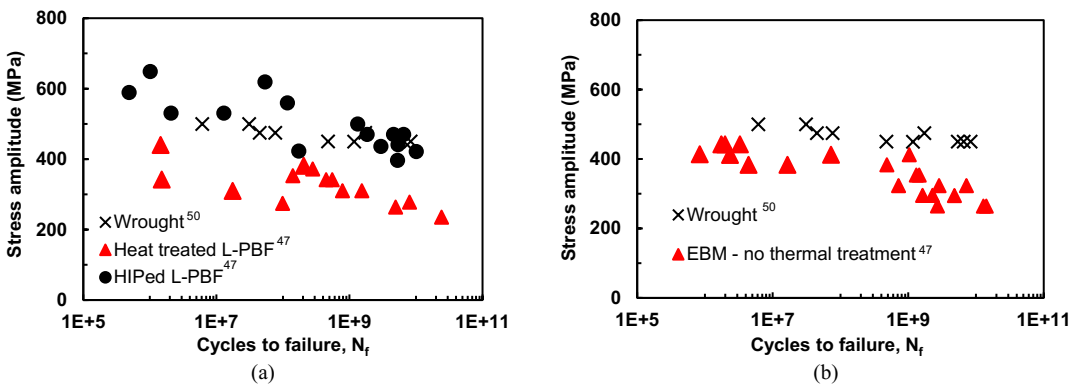


Fig. 4. Comparison of fatigue strengths in high cycle fatigue and very high cycle fatigue regimes with wrought Ti-6Al-4V for (a) L-PBF Ti-6Al-4V, and (b) EBM Ti-64-4V.

4. Summary

The distinct microstructural characteristics of AM parts and the resultant mechanical behaviour are primarily governed by the variations in thermal history, that are ultimately dictated by the process and design parameters. In particular, fatigue is a localized phenomenon in which its failure mechanisms are largely driven from the stress concentration caused by manufacturing-induced defects. Therefore, understanding the correlation between the manufacturing parameters and the manufacturing-induced defect distribution is considered to be an important step to minimize and control these material anomalies within AM parts, which eventually alleviate the scatter in their fatigue resistance.

Depending on the material systems and manufacturing process type, the presence of residual stresses in AM parts can be significant which, in turn, can be beneficial or detrimental to their fatigue resistance. Relative to the AM processes utilizing laser as an energy source, parts fabricated using an electron beam-based process are expected to have lower residual stresses due to the much higher temperature environment during fabrication. Mechanical and thermal treatments such as build platform heating, as well as post-manufacturing machining, shot-peening, and stress-relief heat treatment have been shown to weaken tensile residual stresses. However, these treatments do not always lead to the improved fatigue performance of AM parts. Moreover, depending on the build orientation, the effects of post-manufacturing treatment on fatigue life can vary. Further study is therefore recommended to understand the mechanisms underlying the distinctive effects of post-manufacturing treatment on fatigue strength for AM specimen fabricated in different orientations.

Due to the lack of VHCF studies for AM materials, there is a critical need to obtain the fatigue behavior at gigacycles and the influences of design parameters, size/geometry, surface roughness, etc. An understanding of the fatigue failure mechanism transition from surface to subsurface crack initiation in VHCF for AM parts is not fully realized. In addition, since the fabrication (process parameters) and microstructure (structure) of AM parts dictate their mechanical behaviour (property), it is imperative that all of these phases be taken into consideration. The process-structure-property-performance relationships for AM process and material systems should therefore be established to enable the adoption of AM technology in applications that require the survival of AM parts/systems under very high number of loading cycles.

Acknowledgements

Partial funding for this work was provided by the National Science Foundation under Grant No. 1657195.

References

- 1 Frazier WE. J. Mater. Eng. Per. 23, 6 (2014).
- 2 Murr LE, Gaytan SM, Ramirez DA, Martinez E, Hernandez J, Amato KN, Shindo PW, Medina FR, Wicker RB. J. Mater. Sci. Tech. 28, 1 (2012).
- 3 Shamsaei N, Yadollahi A, Bian L, Thompson SM. Addit. Manuf. 8, (2015).
- 4 Lewandowski JJ, Seifi M. Annu. Rev. Mater. Res. 46 (2016).
- 5 Seifi M, Gorelik M, Waller J, Hrabe N, Shamsaei N, Daniewicz S, Lewandowski JJ. JOM. 69, 3 (2017).
- 6 Romano S, Brandão A, Gumpinger J, Gschweitl M, Beretta S. Mater. Des. 131 (2017).
- 7 Yadollahi A, Shamsaei N. Int. J. Fatigue. 98 (2017).
- 8 Bian L, Thompson SM, Shamsaei N. JOM. 67, 3 (2015).
- 9 Beretta S, Romano S. Int. J. Fatigue. 94 (2017).
- 10 Sterling AJ, Torries B, Shamsaei N, Thompson SM, Seely DW. Mater. Sci. Eng. A. 655 (2016).
- 11 Johnson AS, Shao S, Shamsaei N, Thompson SM, Bian L. JOM. 3, 69 (2016).
- 12 Shrestha S, Simsiriwong J, Shamsaei N, Thompson SM, Bian L. In Solid Freeform Fabrication Proceedings (Austin, TX, 2016), pp. 606-616.
- 13 Li P, Warner DH, Fatemi A, Phan N. Int. J. Fatigue. 85 (2016).
- 14 Yadollahi A, Shamsaei N, Thompson SM, Elwany A, Bian L. Int. J. Fatigue. 94 (2017).
- 15 Shao S, Mahtabi MJ, Shamsaei N, Thompson SM. Comp. Mater. Sci. 131 (2017).
- 16 Atkinson HV, Davies S. Metall. Mater. Trans A. 31, 12 (2000).
- 17 Schajer GS, Practical residual stress measurement methods. (Chichester, West Sussex: John Wiley & Sons Ltd, 2013).
- 18 Mercelis P, Kruth JP. Rapid Prototyp. J. 12, 5 (2006).
- 19 Moat RJ, Pinkerton AJ, Li L, Withers PJ, Preuss M. Mater. Sci. Eng. A. 528, 6 (2011).
- 20 Bussu G, Irving PE. Int. J. Fatigue. 25, 1 (2003).
- 21 Rangaswamy P, Griffith ML, Prime MB, Holden TM, Rogge RB, Edwards JM, Sebring RJ. Mater. Sci. Eng. A. 399, 1 (2005).
- 22 Wu AS, Brown DW, Kumar M, Gallegos GF, King WE. Metall. Mater. Trans A. 45, 13 (2014).
- 23 Dai K, Shaw L. Rapid Prototyp. J. 28, 5 (2002).
- 24 Beuth J, Klingbeil N. JOM. 53, 9 (2001).
- 25 Stephens RI, Fatemi A, Stephens RR, Fuchs HO. Metal fatigue in engineering, 2nd ed. (New York, NY: John Wiley & Sons Ltd, 2000).
- 26 Shiomi M, Osakada K, Nakamura K, Yamashita T, Abe F. CIRP Ann. Manuf. Techn. 53, 1 (2004).
- 27 Leuders S, Lieneke T, Lammers S, Tröster T, Niendorf T. J. Mater. Res. 29, 17 (2014).
- 28 Leuders S, Thöne M, Riemer A, Niendorf T, Tröster T, Richard HA, Maier HJ. Int. J. Fatigue. 48, (2013).
- 29 Zhang H, Chiang R, Qin H, Ren Z, Hou X, Lin D, Doll GL, Vasudevan VK, Dong Y, Ye C. Int. J. Fatigue. 103 (2017).
- 30 Edwards P, O'Conner A, Ramulu M. J. Manuf. Sci. Eng. 135, 6 (2013).
- 31 Facchini L, Magalini E, Robotti P, Molinari A. Rapid Prototyp. J. 15, 3 (2009).
- 32 Hrabe N, Gnäupel-Herold T, Quinn T. Int. J. Fatigue. 94 (2017).
- 33 Mower TM. Int. J. Fatigue. 64 (2014).
- 34 Walker K. ASTM STP 462. (West Conshohocken, PA: American Society for Testing and Materials, 1970).
- 35 Metallic Materials Properties Development and Standardization (MMPDS-05), Battelle Memorial Institute (2010).
- 36 Selcuk C. Powder. Metall. 54, 2 (2011).
- 37 Kruth JP, Deckers J, Yasa E, Wauthlé R. Proc. Inst. Mech. Eng., B. 226, 6 (2012).
- 38 Shuangyin Z, Xin L, Jing C, Weidong H. Rare Metal Mat. Eng. 5 (2009).
- 39 Edwards P, Ramulu M. Mate. Sci. Eng. A. 598 (2014).
- 40 Bathias C, Paris PC. Gigacycle fatigue in mechanical practice, 1st ed. (New York, NY: Marcel Dekker, 2005).
- 41 Wang QY, Lib T, Zenga XG. Procedia Eng. 2, 1 (2010).
- 42 Almaraz GM. Mech. Mater. 40, 8 (2008).
- 43 Mayer H, Haydn W, Schuller R, Issler S, Furtner B, Bacher-Höchst M. Int. J. Fatigue. 31, 2 (2009).
- 44 Boyer HE. Atlas of fatigue curves. (Materials Park, OH:ASM International, 1985).
- 45 Mayer H. Fatigue Fract. Eng. M. 39, 1 (2016).
- 46 Siddique S, Imran M, Wycisk E, Emmelmann C, Walther F. Mater. Today Proc. 3, 9 (2016).
- 47 Günther J, Krewerth D, Lippmann T, Leuders S, Tröster T, Weidner A, Biermann H, Niendorf T. Int. J. Fatigue. 94 (2017).
- 48 Siddique S, Imran M, Walther F. Int. J. Fatigue. 94 (2017).
- 49 Krewerth D, Weidner A, Biermann H. Ultrasonics. 2013;53(8):1441-9.
- 50 Janeček M, Nový F, Harcuba P, Stráský J, Trško L, Mhaede M, Wagner L. Acta Phys. Pol. A.128, 4 (2015).
- 51 Bayraktar E, Garcias IM, Bathias C. Int. J. Fatigue. 28, 11 (2006).